Chemistry and Materials

The Center for Science Innovation

Tab Research Article

Chem. Mater. 3 (3) 2024, 71-79

Methylene Blue Photodegradation Using Cu-decorated Cu_2O Prepared by a Facile Electrochemical Deposition Method

Shyla Noureen Zahra[1], Firgie Wulandari[1], Muhammad Raihan Rauf[2], Arum Ayuningsih[3,*]

[1]Department of Chemistry, Faculty of Mathematics and Natural Science, Universitas Negeri Jakarta, Jalan Rawamangun Muka, Jakarta 13220, Indonesia

[2]The Center for Science Innovation, Jakarta 13120, Indonesia

[3]Department of Materials Science and Engineering, Chonnam National University, 300 Yongbong-dong, Buk-gu, Gwangju 61186, Republic of Korea

*Corresponding author: arumayu@jnu.ac.kr

Received
13 August 2024

Received in revised form
9 October 2024

Accepted
19 October 2024

Published online
31 October 2024

DOI
https://doi.org/10.56425/cma.v3i3.81

Abstract

A cuprous oxide (Cu_2O) thin film was decorated with copper metal (Cu) using a simple electrochemical deposition method on a substrate of indium tin oxide at a potential of -0.3 V vs. Ag/AgCl and a temperature of 60 °C. This study aimed to investigate the role of Cu as a co-catalyst. The structure, phase, and morphology of Cu_2O/Cu were characterized by X-ray diffraction, scanning electron microscopy, and energy-dispersive X-ray spectroscopy, respectively. The electrocatalytic performance of Cu_2O/Cu was recorded using linear sweep voltammetry and electrochemical impedance spectroscopy techniques. The X-ray diffraction and scanning electron micrograph show that Cu was successfully deposited covering Cu_2O. The current density of Cu_2O/Cu increased by 2.70 mA/cm^2 confirming the lower charge current resistance of 2.48 kΩ. The Cu-decorated Cu_2O demonstrated an improved photocatalytic activity, as shown by increased MB degradation from 46.33% to 50.87%. It was believed from characterizations that Cu deposition leads to more dense carriers and charge transfer, hence higher photocatalytic activity towards MB degradation than bare Cu_2O thin film.

Keywords: photocatalyst, photodegradation, non-noble metal, co-catalyst, Cu_2O

1. Introduction

Nanotechnology has been a rapidly growing field of research in recent decades, with wide potential applications across various sectors, including the environment. One environmental issue that is currently the focus of significant attention is water pollution caused by effluents. The textile industry, for instance, generates a large volume of wastewater containing synthetic dyes such as Methylene Blue, a known toxic and carcinogenic pollutant [1]. Methylene Blue (MB) is a heterocyclic aromatic chemical compound with a planar structure, making it part of complex compounds that are difficult for nature to biodegrade. Waste containing organic pollutants, particularly MB, is often discharged directly into water bodies without adequate treatment, leading to serious pollution and negative impacts on ecosystems and human health [2-4]. Various methods have been proposed to address this problem, including adsorption [5-7], filtration [8–10], catalytic oxidation [11,12] and chemical precipitation [13]. However, these methods are often ineffective due to limitations such as toxicity, production of secondary pollutants, and high operating costs [5]. The limitations of these methods highlight the need to explore other effective approaches that are both highly efficient and economically viable.

Photocatalytic processes involving semiconductor catalysts can be the solution to the appropriate method for decomposing MB waste that has been present in water bodies. The process can significantly increase the reaction rate to achieve optimal degradation efficiency. However, some factors are still considered in using this method, including the band gap energy of the photocatalyst

material used, the rate of charge recombination, crystal structure, and surface roughness [15,16]. Several semiconductor materials have been studied and successfully used as the main material in photocatalysts, including $ZnWO_4$ [17], TiO2 [18], ZnO [19], ZnS [20], Bi_2WO_6 [21], $BiVO_4$ [22], Fe_2O_3 [23], and Cu_2O [24]. Currently, semiconductor materials, particularly those based on copper(I) oxide (Cu_2O), have garnered attention for use as the primary material in photocatalysts due to their ability to degrade organic pollutants in wastewater through photocatalytic reactions [25].

Cu_2O is a p-type semiconductor that is environmentally friendly, has unique electrical properties is non-toxic, and is abundant in nature [26,27]. However, Cu_2O has a narrow band gap energy of approximately 1.2 eV to 2.18 eV, which results in rapid electron recombination and consequently low photocatalytic efficiency [28]. Several approaches began to be used to be able to increase the efficiency of the photocatalytic activity of Cu_2O such as the addition of doping [29], metal modification [30], semiconductor composite [31], structural control [32], and heterostructure [33] as well as by combining metal oxide co-catalysts [34]. It is known that the Cu_2O/noble metal structure is one of the promising candidates to lift photocatalyst efficiency because it can suppress the occurrence of charge recombination [35]. In addition, it has also been proven that efficiency can be improved by utilizing the synergistic effect of surface plasma resonance [36–38].

However, non-noble metal co-catalysts, such as Cu-based photocatalysts, are favoured due to the high cost and limited availability of precious metals. Non-noble metal co-catalysts, such as Cu, are highly active, stable, and inexpensive, and can also facilitate the transfer of excited electrons to the Cu (or Cu_2O) surface without the Schottky barrier [39]. This rationale underpins the incorporation of Cu co-catalysts to boost the catalytic activity of Cu_2O. Several methods have been widely used in the synthesis of Cu_2O, including hydrothermal [40], chemical vapour deposition [41], and electrodeposition methods [42]. The electrodeposition method has attracted much attention due to its advantages, such as cost-effectiveness, energy efficiency, ease of synthesis, and environmental compatibility [43].

In this paper, to overcome the disadvantages of Cu_2O, a Cu_2O/Cu thin film was synthesised using the electrodeposition method for MB photodegradation, to explore the role of Cu as a non-noble co-catalyst. MB synthetic dyes were selected due to their exceptional stability, which makes them difficult to degrade naturally [44]. By introducing Cu into the Cu_2O thin film, the MB degradation efficiency was increased, which is consistent with its photoelectrochemical properties. Therefore, this report may contribute to the development of new types of photocatalysts for wastewater treatment applications.

2. Materials and Method

2.1 Materials

Materials such as copper(II) sulphate pentahydrate ($CuSO_4 \cdot 5H_2O$), sodium sulphate (Na_2SO_4), lactic acid ($C_3H_6O_3$), sodium hydroxide (NaOH) and indium tin oxide (ITO), as the substrate, were used in this experiment. All solutions were prepared with distilled water.

2.2 Synthesis of Cu_2O and Cu_2O/Cu

The electrochemical deposition procedure was performed using a potentiostatic technique in a three-electrode cell with ITO as the working electrode, Ag/AgCl (with 3 M KCl) as the reference electrode, and platinum (Pt) foil as the counter electrode. Before electrochemical deposition, the 3 × 2 cm^2 ITO substrate was thoroughly cleaned. The cleaning process involved sequential rinsing with distilled water, ethanol, and distilled water. This sequence was performed twice to ensure optimal cleanliness. Each liquid was carefully dispensed onto the substrate using a squeeze bottle to prevent contamination.

The electrochemical deposition procedure was performed using a potentiostatic technique in a three-electrode cell with ITO as the working electrode, Ag/AgCl (with 3 M KCl) as the reference electrode, and platinum (Pt) foil as the counter electrode. Before electrochemical deposition, the 3 × 2 cm^2 ITO substrate was thoroughly cleaned. The cleaning process involved sequential rinsing with distilled water, ethanol, and distilled water. This sequence was performed twice to ensure optimal cleanliness. Each liquid was carefully dispensed onto the substrate using a squeeze bottle to prevent contamination.

Cu_2O was carried out for 1 h with a potential of –0.3 V and a temperature of 60 °C controlled by Corrtest CS310 workstation using 25 mL of 0.025 M $CuSO_4$. The solution was prepared by stirring 0.156 g of $CuSO_4 \cdot 5H_2O$ and 6.3 mL of lactic acid in a 100 mL beaker glass with a magnetic bar. The magnetic stirrer (DLAB MS-H280-Pro) was turned on at 390 rpm for 20 minutes to obtain a homogenous solution. Afterwards, the pH of the electrolyte solution was adjusted with 10 M NaOH to a pH value of 10.00.

2.3 Characterization

A Thermo Fisher Scientific Quattro S scanning electron microscope (SEM) was used to investigate and analyze the surface morphology of Cu_2O/Cu thin film, coupled to an

EDAX Ametek energy dispersive X-ray analyzer (EDX) to examine the composition of Cu_2O/Cu deposited on ITO. Additionally, the crystal structure of Cu_2O/Cu nanoparticles was characterized using a PANalytical AERIS X-ray diffractometer (XRD).

2.4 Photoelectrochemical test

The photoelectrochemical properties of Cu_2O/Cu were evaluated by electrochemical impedance spectroscopy (EIS) and linear sweep voltammetry (LSV) techniques using a calibrated AM 1.5 G radiation solar simulator from a halogen lamp at an intensity of 100 mW/cm^2 (1 Sun). The tests were carried out in 0.5 M Na_2SO_4 solution controlled by Corrtest CS310 workstation with a conventional three-electrode system, in which the sample@ITO as the working electrode, Ag/AgCl (with 3 M KCl) as the reference electrode, and platinum foil as the counter electrode. The EIS tests were performed at the frequency region from 0.1 Hz to 100 kHz. The photocurrent responses were recorded by scanning the potential from 0.1 V to 0.5 V vs. Ag/AgCl at room temperature, and a scan rate of 50 mV/s [45].

2.5 Photodegradation test

The photocatalytic activity was studied by irradiating visible light to 5 ppm of MB solution by adding Cu_2O or Cu_2O/Cu thin film. Measurement data were collected at 5 minute intervals up to 30 minutes, then at 10 minute intervals up to 120 minutes. The concentrations were monitored using UV-Vis spectrophotometry (GB Cintra 2020) to observe the shifts resulting from the photodegradation of the MB solution [46]. The degradation efficiency was calculated using Equation 1.

$$\text{Degradation efficiency} = \frac{C_0 - C}{C_0} \times 100\% \quad (1)$$

Where C_0 represents the initial concentration and C denotes the concentration measured at specified irradiation times.

3. Results and Discussion

3.1 Structure, phase, and morphology

Figure 1 displays the XRD patterns of Cu_2O and Cu-decorated Cu_2O. The Cu_2O sample exhibits peaks attributed to Cu_2O, with diffraction peaks at 2θ values of 36.24°, 42.00°, 61.27°, and 73.42°, corresponding to the (111), (200), (220), and (311) planes of Cu_2O, respectively [45]. The intensity of these peaks suggests that Cu_2O has a cubic structure, with the (111) plane being far more dominant than the other crystal planes, similar to the XRD pattern reported by Tezcan et al. [47]. For the Cu_2O/Cu sample, both Cu and Cu_2O are detected, with a peak at 2θ of 43.11° corresponding to the (111) plane of cubic Cu [48,49]. After deposition, no observable shifts in the Cu_2O diffraction peaks, indicating that Cu atoms load onto the surface of Cu_2O rather than interstitially distorting the Cu_2O lattice [49,50].

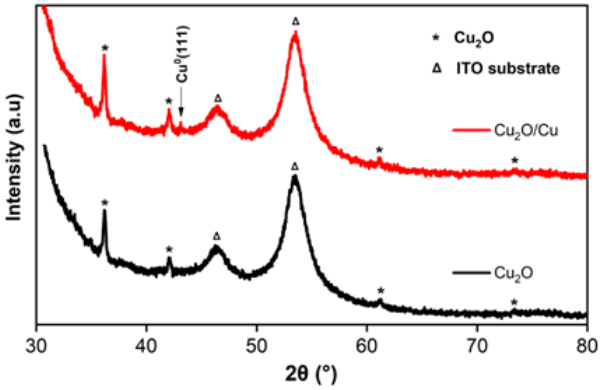

Figure 1. XRD diffractograms of Cu_2O and Cu_2O/Cu.

Understanding the formation of Cu_2O and the coating process of metallic Cu is essential for distinguishing between Cu nanoparticles embedded within Cu_2O (Cu^+) and the Cu metal (Cu) deposited on the Cu_2O thin film. This knowledge is critical for identifying the unique properties and interactions of these nanoparticles within the material. Ait Hssi et. al. [51] reported a LSV study of Cu_2O on FTO substrates deposited from 0.2M $CuSO_4$ and 3 M lactic acid with a pH of 9 at 60 °C. It is known that two reduction reactions undergo for Cu^{2+} ions, first Cu^{2+} into Cu^+ (Eqn. 2), formed Cu^+ ions then react with the OH^- ions in the solution to form the Cu_2O (Eqn. 3). Secondly, Cu^0 nanoparticles are formed from the reduction of Cu^+ ions, which do not get to bond with OH^- (Eqn. 4) [52,53].

$$Cu^{2+}{}_{(aq)} + e^- \leftrightarrow Cu^+{}_{(aq)} \quad (2)$$

$$2Cu^+{}_{(aq)} + 2OH^-{}_{(aq)} \leftrightarrow Cu_2O_{(s)} + H_2O_{(l)} \quad (3)$$

$$Cu^{2+}{}_{(aq)} + 2e^- \leftrightarrow Cu^o{}_{(s)} \quad (4)$$

The surface morphology of Cu_2O and Cu_2O/Cu is shown in the SEM micrographs in Fig. 2. It is evident Cu deposition alters the surface morphology of the Cu_2O thin film. The formed thin films consist of an aggregation of smaller nanoparticles distributed uniformly. Depositing Cu from a 0.025 M $CuSO_4$ solution at –0.3 V onto Cu_2O made the grain boundaries of the aggregated Cu_2O nanoparticles more noticeable. The thin films have average grain sizes of 378 nm and 309 nm, as determined by manual particle size analysis using ImageJ software, for Cu_2O and Cu_2O/Cu thin films, respectively. The difference in average grain sizes could be due to the presence of Cu, which is relatively smaller, covering the surface of Cu_2O [50].

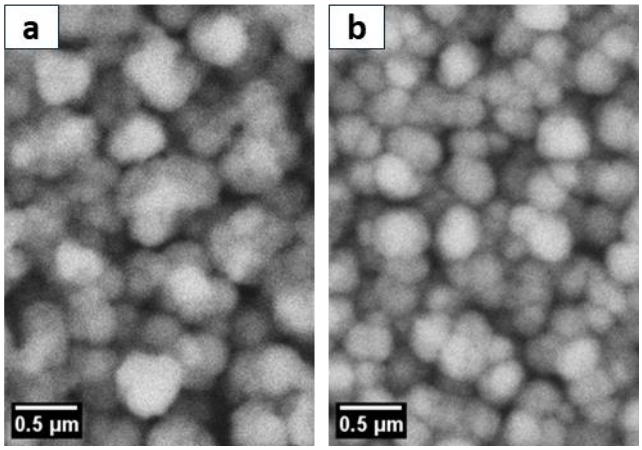

Figure 2. SEM micrograph of the Cu_2O and Cu_2O/Cu.

XRD analysis confirmed that no Cu peak was observed in the Cu_2O thin film, suggesting that the higher Cu content in Cu_2O/Cu can be attributed to adding Cu to the overall Cu atomic ratio. The coating process of Cu onto the Cu_2O thin film is believed to follow the reaction shown in Eqn. 4, as there are no OH^- ions available to bond within the 0.025 M $CuSO_4$ solution, which is acidic with a pH value of around 5 [39]. This result aligns with Cheng et. al. (2016) report on Cu-Cu_2O nanocomposites, where the size of Cu_2O microspheres decreases while the size of Cu nanoparticles increases as the reaction progresses [41]. The atomic ratio of Cu in the thin films, as measured by EDX, is 31.7% and 44.0% for Cu_2O and Cu_2O/Cu, respectively. The EDX results indicate that Cu content increases with the addition of Cu onto the surface of Cu_2O, thereby confirming the deposition of Cu in Cu_2O/Cu. The SEM-EDX results are consistent with the observations from the XRD analysis that Cu-decorated Cu_2O thin film was successfully obtained.

3.2 Electrochemical impedance analysis

The Nyquist diagram (Z imaginary versus Z real) from Cu_2O and Cu_2O/Cu under irradiation, shown in Fig. 3, are the results of EIS measurements. These plots show straight lines in the low-frequency range and semicircles in the high-frequency range, indicating the mass and transfer resistivity of the electrolyte and the presence of total charge transfer resistance (R_{ct}), respectively [14]. It was observed from Fig. 3 and Table 1 that the diameter of the semicircle of Cu_2O/Cu is shorter with an R_{ct} of 10.80 Ω than that of Cu_2O, which has an R_{ct} of 21.46 Ω. The lower R_{ct} value for Cu_2O/Cu indicates an easier charge transfer resulting in a more charge-abundant interface confirmed by the elevated R_s value from 29.78 Ω to 34.23 Ω [45]. This result also implies that Cu_2O/Cu is more conductive, it opens the possibility of a narrower bandgap. Similar observations have been noted where Cu deposition on certain materials did not significantly alter the bandgap [40]. This suggests that the Cu co-catalyst may be predominantly confined to the surface of the substrate, enhancing surface charge density without impacting the intrinsic bandgap of the material.

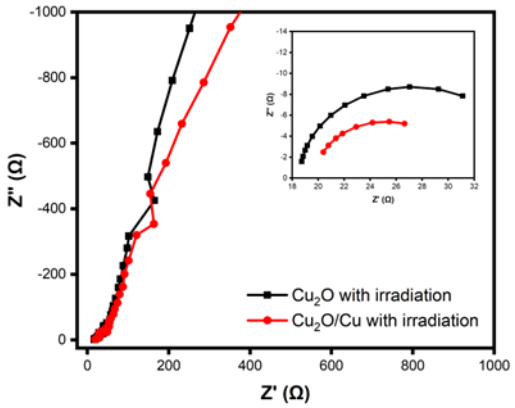

Figure 3. Nyquist plots were measured with irradiation for Cu_2O and Cu_2O/Cu.

Table 1. Solution resistance (R_s) and charge transfer resistance (R_{ct}) value from EIS measurement.

Sample	R_s (Ω)	R_{ct} (Ω)
Cu_2O	29.781	10369
Cu_2O/Cu	34.234	2488

3.3 Photoelectrochemical analysis

The photoelectrochemical (PEC) test was conducted to assess the impact of Cu decoration. This PEC measurement aimed to record the photocurrent densities of Cu_2O and Cu_2O/Cu. Figure 4 shows LSV curves that illustrate the relationship between voltage and photocurrent density for the photocatalyst materials, both with and without irradiation. According to the results presented in Fig. 4, the photocurrent density of bare Cu_2O reaches 1.73 mA/cm² at a potential of 0.30 V vs. Ag/AgCl. After the deposition of the Cu co-catalyst, this photocurrent density increases to 2.70 mA/cm² at a potential of 0.40 V vs. Ag/AgCl. Thus, it can be concluded that Cu_2O with Cu has a higher photocurrent density than Cu_2O alone. This enhancement occurs because Cu, as a co-catalyst, effectively reduces the recombination of electron-hole pairs caused by the narrow band gap energy of Cu_2O. Additionally, Cu improves the trapping of photoexcited electrons, further boosting the photocatalytic performance [46].

The PEC flat response recorded without irradiation implies that the photocurrent enhancement gain generated by Cu_2O and Cu_2O/Cu was from the formation

of photoexcited electron (e^-) and hole (h^+) pairs driven by the adsorbed photons under visible light illumination [48,54]. This result is consistently in line with and confirms the EIS results. Decorating Cu on Cu_2O led to an increase in electron-hole density on the surface, which is the spot where the photocatalytic activities will occur [48]. Thus, it is proven that the deposition of Cu co-catalyst on Cu_2O shows a good synergistic effect and better influences MB degradation than bare Cu_2O.

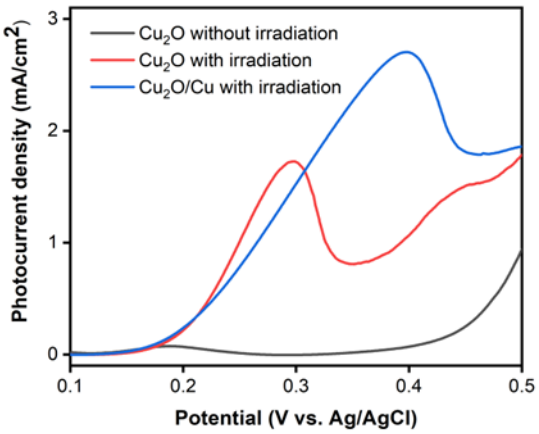

Figure 4. Photocurrent responses without and with irradiation for Cu_2O and Cu_2O/Cu.

3.4 Photocatalytic degradation of methylene blue

The reduced concentration (conc.) of MB after 2 h of irradiation in the presence of Cu-decorated Cu_2O when subjected to visible light. Based on the UV-Vis spectra shown in Fig. 5. indicating the degradation of MB, the intensity of absorbance peaks decreases meaning a more reduced concentration of MB. It was observed that MB has an absorption peak at 664.24 nm whose intensity reduces over irradiation time [41]. Figure 6. presents the degradation efficiency of the MB solution, showing that Cu holds a role in improving the photocatalytic activity of Cu_2O from 43.66% to 50.87%. The high percentage value of degradation efficiency achieved in the photocatalytic activity of Cu_2O/Cu thin films is due to the much larger surface area possessed by the Cu-added thin films, which is also related to the low average grain size produced based on SEM analysis results. Thus, the smaller the particle size, the greater of surface area owned by the thin film [49]. Besides that, of course, surface area has a major role in photocatalysts, so that with increasing surface area, the activity of photocatalysts in MB degradation will also increase. This is because the contact area between the photocatalyst and the target material will be much larger, which then has an impact on the high level of UV absorption and the percentage value degradation efficiency which is also high [50].

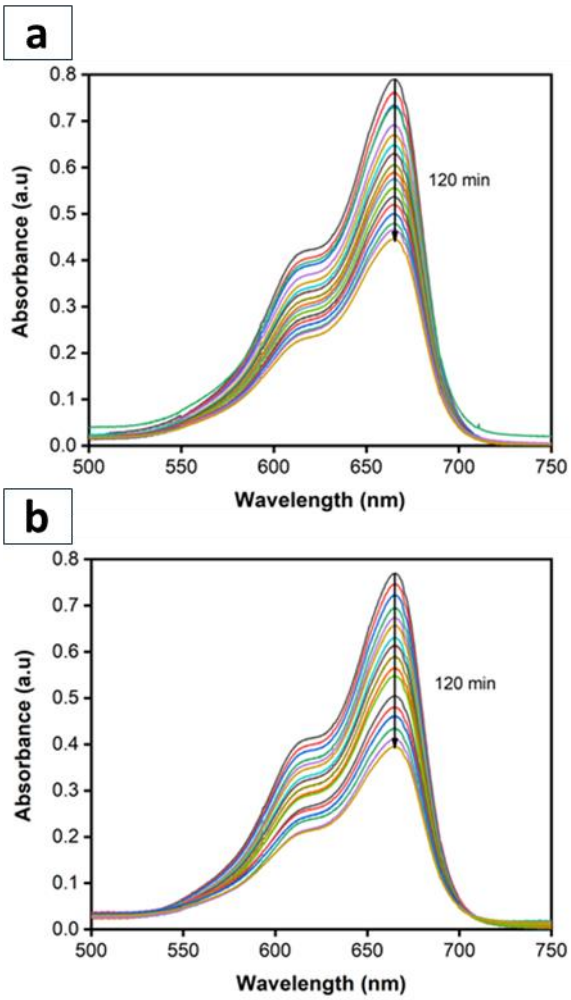

Figure 5. UV-Vis absorbance spectra of (a) Cu_2O and (b) Cu_2O/Cu.

Photocatalysts when exposed to irradiation will absorb photon energy, which generates a photoexcited electron (e^-) in the conduction band (CB) and a hole (h^+) in the valence band (VB). The photoexcited electrons in Cu_2O can be more efficiently transferred to the dispersed Cu on the surface because of the low work function and good conductive ability that was validated by EIS analysis [41,51]. This results in low charge carriers recombination since the introduction of Cu will further raise the VB of Cu_2O [41]. The photogenerated electrons and holes facilitate photocatalytic reactions to form oxidative radicals. These oxidative radicals react with the MB compounds, thereby exhibiting strong redox capabilities and increasing the photodegradation efficiency of MB.

The raised VB of Cu_2O makes it higher than the oxidation potential of water (H_2O), preventing the holes from reacting with OH- to form hydroxyl radicals (•OH), essential for breaking down MB. Additionally, the dissolved oxygen in water is insufficient to effectively produce superoxide radicals ($•O^{2-}$), which are also crucial for the

degradation process. Consequently, due to the lack of generation of these reactive oxidative species, the Cu_2O/Cu photocatalyst may need further development for more extra photocatalytic activity [40,41].

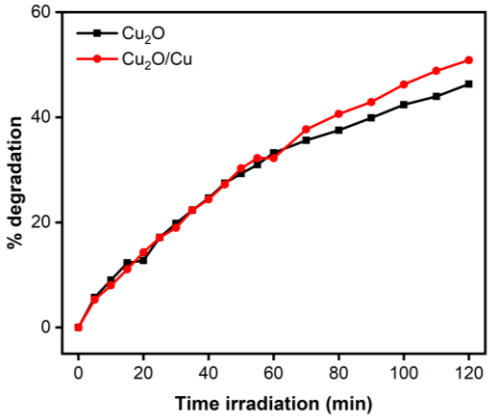

Figure 6. Photodegradation of MB using Cu_2O or Cu_2O/Cu.

A plausible explanation for the stability of the photocatalytic properties is that both Cu metal and Cu_2O exhibit activity under visible light [55]. Photocatalytic reactions occur under required circumstances, like appropriate energy band potential (including the demands of band gap and energy band potential) and abundant active sites on the photocatalyst's surface [49]. Therefore, the Cu metal nanoparticles on Cu_2O thin film play a role in photocatalytic properties in the following ways: (1) EIS results show the relatively low resistance of Cu_2O/Cu is convenient for the photoexcited electron transfer; (2) PEC analysis indicates that the Cu metal nanoparticles are electron storage centers, which facilitate charge separation in the photocatalyst; (3) the higher Cu_2O/Cu degradation efficiency shows the contribution to photocatalytic property under visible light.

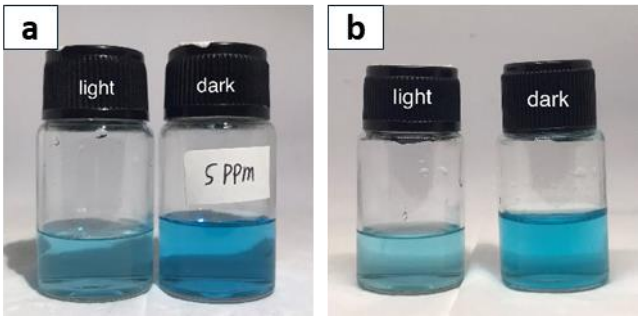

Figure 7. Color change of MB solution photodegradation (a) using Cu_2O; (b) with Cu_2O/Cu photocatalysts.

4. Conclusion

The Cu-decorated Cu_2O photocatalyst was successfully synthesized via electrodeposition on an ITO substrate for MB photodegradation. The degradation experiments revealed that the presence of Cu as a co-catalyst on Cu_2O improved the photodegradation efficiency from 46.33% to 50.87% under visible light irradiation. Additionally, by examining the photocatalytic activity under a specific wavelength of incident light (664.24 nm), it was confirmed that Cu significantly enhances the performance of the photocatalyst. The Cu co-catalyst likely acts as a receptor for photoexcited electrons, enhancing charge separation and preventing electron-hole pair recombination. This increased separation boosts the number of electrons available to initiate reduction and oxidation reactions involving the adsorbed species on the surface, as supported by the photocurrent responses and EIS Nyquist plots.

Acknowledgement

This work was supported by The Ministry of Education, Culture, Research, and Technology, Indonesia (Grant number: 2/UN39.14/PG.02.00.PL/PT/VI/2024).

References

[1] C. Retamoso, N. Escalona, M. González, L. Barrientos, P. Allende-González, S. Stancovich, R. Serpell, J.L.G. Fierro, M. Lopez, Effect of particle size on the photocatalytic activity of modified rutile sand (TiO2) for the discoloration of methylene blue in water, *J Photochem Photobiol A Chem*. **378** (2019) 136–141. https://doi.org/10.1016/j.jphotochem.2019.04.021.

[2] S. Velusamy, A. Roy, S. Sundaram, T. Kumar Mallick, A Review on Heavy Metal Ions and Containing Dyes Removal Through Graphene Oxide-Based Adsorption Strategies for Textile Wastewater Treatment, *The Chemical Record*. **21** (2021) 1570–1610. https://doi.org/10.1002/TCR.202000153.

[3] W.U. Khan, S. Ahmed, Y. Dhoble, S. Madhav, A critical review of hazardous waste generation from textile industries and associated ecological impacts, *Journal of the Indian Chemical Society*. **100** (2023) 100829.https://doi.org/10.1016/J.JICS.2022.100829.

[4] K. Sharma, S. Rajan, S.K. Nayak, Water pollution: Primary sources and associated human health hazards with special emphasis on rural areas, *Water Resources Management for Rural Development*. (2024) 3–14. https://doi.org/10.1016/B978-0-443-18778-0.00014-3.

[5] S.A. Ong, E. Toorisaka, M. Hirata, T. Hano, Biodegradation of redox dye Methylene Blue by up-flow anaerobic sludge blanket reactor, *J Hazard Mater*. **124** (2005) 88–94. https://doi.org/10.1016/J.JHAZMAT.2005.03.054.

[6] S.R. Geed, K. Samal, A. Tagade, Development of adsorption-biodegradation hybrid process for removal of methylene blue from wastewater, *J Environ Chem Eng*. **7** (2019) 103439. https://doi.org/10.1016/J.JECE.2019.103439.

[7] H.S. Kusuma, D.E. Christa Jaya, N. Illiyanasafa, K.L. Ikawati, E. Kurniasari, H. Darmokoesoemo, A.N. Amenaghawon, A critical review and bibliometric analysis of methylene blue adsorption using leaves, *Chemosphere*. **356** (2024) 141867. https://doi.org/10.1016/J.CHEMOSPHERE.2024.141867.

[8] S. De Gisi, G. Lofrano, M. Grassi, M. Notarnicola, Characteristics and adsorption capacities of low-cost sorbents for wastewater treatment: A review, *Sustainable Materials and Technologies*. **9** (2016) 10–40. https://doi.org/10.1016/J.SUSMAT.2016.06.002.

[9] E. Pramono, G.P.W. Sejati, S. Wahyuningsih, C. Purnawan, Polyvinylidene Fluoride (PVDF)/Modified Clay Hybrid Membrane for Humic Acid and Methylene Blue Filtration, *Indonesian Journal of Chemistry*. **23** (2023) 425–437. https://doi.org/10.22146/IJC.78979.

[10] X. Shao, J. Wang, Z. Liu, N. Hu, M. Liu, C. Duan, R. Zhang, C. Quan, Cellulose based cation-exchange fiber as filtration material for the rapid removal of methylene blue from wastewater, *Cellulose*. **28** (2021) 9355–9367. https://doi.org/10.1007/S10570-021-04103-2/METRICS.

[11] J. Wu, Q. Ma, P. Li, Z. Wan, X. Peng, An Innovative Asymmetric Polyethersulfone Membrane Containing Chitosan and Cellulose Nanofibrils with a Compact Crosslinking Structure for Methyl Blue Filtration, *SSRN*. (2024) 136. https://doi.org/10.2139/SSRN.4737679.

[12] M.J. Ndolomingo, R. Meijboom, Kinetic analysis of catalytic oxidation of methylene blue over γ-Al2O3 supported copper nanoparticles, *Appl Catal A Gen*. **506** (2015) 33–43. https://doi.org/10.1016/J.APCATA.2015.08.036.

[13] A. Kuntubek, N. Kinayat, K. Meiramkulova, S.G. Poulopoulos, J.C. Bear, V.J. Inglezakis, Catalytic Oxidation of Methylene Blue by Use of Natural Zeolite-Based Silver and Magnetite Nanocomposites, *Processes 2020, Vol. 8, Page 471*. **8** (2020) 471. https://doi.org/10.3390/PR8040471.

[14] Y.T. Gaim, G.M. Tesfamariam, G.Y. Nigussie, M.E. Ashebir, Synthesis, characterization and photocatalytic activity of n-doped cu2o/zno nanocomposite on degradation of methyl red, *Journal of Composites Science*. **3** (2019). https://doi.org/10.3390/jcs3040093.

[15] L. Wang, M. Tang, H. Jiang, J. Dai, R. Cheng, B. Luo, L. Yang, G. Du, W. Gao, Sustainable, efficient, and synergistic photocatalytic degradation toward organic dyes and formaldehyde gas via Cu2O NPs@wood, *J Environ Manage*. **351** (2024) 119676. https://doi.org/10.1016/J.JENVMAN.2023.119676.

[16] M.G. Sutrisno, Yusmaniar, A.M. Noor, S. Budi, Electrodeposition of Zn-Doped Cu2O-Cu/Ni for methylene blue photodegradation, in: J Phys Conf Ser, Institute of Physics, 2023. https://doi.org/10.1088/1742-6596/2596/1/012017.

[17] N.T.T. Mai, M.M. Neto, P. Van Thang, N.N. Trung, N.C. Tu, T.N. Dung, H.D. Chinh, L.T.L. Anh, Cu2O Nanoparticles: A simple synthesis, characterization and its photocatalytic performance toward methylene blue, *Mater Trans*. **61** (2020) 1868–1873. https://doi.org/10.2320/matertrans.MT-MN2019039.

[18] W. Zhang, X. Li, Z. Yang, X. Tang, Y. Ma, M. Li, N. Hu, H. Wei, Y. Zhang, *In situ* preparation of cubic Cu $_2$ O-RGO nanocomposites for enhanced visible-light degradation of methyl orange, *Nanotechnology*. **27** (2016) 265703. https://doi.org/10.1088/0957-4484/27/26/265703.

[19] L. Zhang, X. Wang, Photocatalytic performance of Cu2O and Ag/Cu2O composite octahedra prepared by a propanetriol-reduced process, *Applied Physics A*. **117** (2014) 2189–2196. https://doi.org/10.1007/s00339-014-8644-4.

[20] D.S.D. Lima, J.C. Cruz, V.A. Luciano, M.A. Nascimento, A.P.C. Teixeira, R.P. Lopes, Enhanced photocatalytic activity of cobalt-doped titanate nanotube heterostructures decorated with Cu2O-CuO nanoparticles for organic pollutant degradation under UV and visible irradiation, *Appl Surf Sci*. **563** (2021). https://doi.org/10.1016/j.apsusc.2021.150313.

[21] X. Yu, J. Zhang, Y. Chen, Q. Ji, Y. Wei, J. Niu, Z. Yu, B. Yao, Ag-Cu2O composite films with enhanced photocatalytic activities for methylene blue degradation: Analysis of the mechanism and the degradation pathways, *J Environ Chem Eng*. **9** (2021)

106161.
https://doi.org/10.1016/j.jece.2021.106161.

[22] S.-T. Guo, Z.-Y. Tang, Y.-W. Du, T. Liu, T. Ouyang, Z.-Q. Liu, Chlorine anion stabilized Cu2O/ZnO photocathode for selective CO2 reduction to CH4, *Appl Catal B*. **321** (2023) 122035. https://doi.org/10.1016/j.apcatb.2022.122035.

[23] H. Xu, W. Wang, W. Zhu, Shape Evolution and Size-Controllable Synthesis of Cu $_2$ O Octahedra and Their Morphology-Dependent Photocatalytic Properties, *J Phys Chem B*. **110** (2006) 13829–13834. https://doi.org/10.1021/jp061934y.

[24] Y. Lou, Y. Zhang, L. Cheng, J. Chen, Y. Zhao, A Stable Plasmonic Cu@Cu $_2$ O/ZnO Heterojunction for Enhanced Photocatalytic Hydrogen Generation, *ChemSusChem*. **11** (2018) 1505–1511. https://doi.org/10.1002/cssc.201800249.

[25] S. Budi, D. Indrawati, M. Arum, Yusmaniar, Electrodeposition and photoelectrochemical response of Zn-doped Cu2O, in: AIP Conf Proc, American Institute of Physics Inc., 2021. https://doi.org/10.1063/5.0045470.

[26] Y. Zheng, C. Chen, Y. Zhan, X. Lin, Q. Zheng, K. Wei, J. Zhu, Photocatalytic Activity of Ag/ZnO Heterostructure Nanocatalyst: Correlation between Structure and Property, *The Journal of Physical Chemistry C*. **112** (2008) 10773–10777. https://doi.org/10.1021/jp8027275.

[27] S. Navalon, M. de Miguel, R. Martin, M. Alvaro, H. Garcia, Enhancement of the Catalytic Activity of Supported Gold Nanoparticles for the Fenton Reaction by Light, *J Am Chem Soc*. **133** (2011) 2218–2226. https://doi.org/10.1021/ja108816p.

[28] H. Zhu, X. Ke, X. Yang, S. Sarina, H. Liu, Reduction of Nitroaromatic Compounds on Supported Gold Nanoparticles by Visible and Ultraviolet Light, *Angewandte Chemie International Edition*. **49** (2010) 9657–9661. https://doi.org/10.1002/anie.201003908.

[29] Y. Pan, S. Deng, L. Polavarapu, N. Gao, P. Yuan, C.H. Sow, Q.-H. Xu, Plasmon-Enhanced Photocatalytic Properties of Cu $_2$ O Nanowire–Au Nanoparticle Assemblies, *Langmuir*. **28** (2012) 12304–12310. https://doi.org/10.1021/la301813v.

[30] J. Zhu, G. Cheng, J. Xiong, W. Li, S. Dou, Recent Advances in Cu-Based Cocatalysts toward Solar-to-Hydrogen Evolution: Categories and Roles, *Solar RRL*. **3** (2019). https://doi.org/10.1002/solr.201900256.

[31] B. Yuan, X. Liu, H. Fu, J. Liu, Q. Zhu, M. Wu, One-step synthesis of flower-like Cu2O photoelectric materials by hydrothermal method, *Solar Energy*. **188** (2019) 265–270. https://doi.org/10.1016/j.solener.2019.06.014.

[32] G.-F. Pan, S.-B. Fan, J. Liang, Y.-X. Liu, Z.-Y. Tian, CVD synthesis of Cu $_2$ O films for catalytic application, *RSC Adv*. **5** (2015) 42477–42481. https://doi.org/10.1039/C5RA05635G.

[33] S. Budi, W.A. Adi, Yusmaniar, Z. Fairuza, I. Basori, A.A. Umar, Structural Analysis of Nanocrystalline Cu2O Prepared by Electrodeposition at Different Temperatures, *Int J Electrochem Sci*. **17** (2022). https://doi.org/10.20964/2022.03.08.

[34] S. Budi, D.I. Syafei, Yusmaniar, Q.F. Khasanah, D. Laxmianti, Electrodeposition of CU2O Films at Room Temperature for Methylene Blue Photodegradation, in: J Phys Conf Ser, Institute of Physics, 2022. https://doi.org/10.1088/1742-6596/2377/1/012004.

[35] M.R. Dustgeer, S.T. Asma, A. Jilani, K. Raza, S.Z. Hussain, M.B. Shakoor, J. Iqbal, M.Sh. Abdel-wahab, R. Darwesh, Synthesis and characterization of a novel single-phase sputtered Cu2O thin films: Structural, antibacterial activity and photocatalytic degradation of methylene blue, *Inorg Chem Commun*. **128** (2021) 108606. https://doi.org/10.1016/j.inoche.2021.108606.

[36] S. Budi, M.G. Sutrisno, Y. Pratiwi, N. Yusmaniar, Enhanced photocatalytic activity of CoNi-decorated Zn-doped Cu2O synthesized by electrodeposition technique, *Mater Adv*. **4** (2023) 1081–1088. https://doi.org/10.1039/D2MA00916A.

[37] M. Athariq, M.R. Rauf, I.W. Khairany, I.F. Adani, M.G. Sutrisno, Synthesis and Characterization of Nanocube Cu2O Thin Film at Room Temperature for Methylene Blue Photodegradation Application, *Chemistry and Materials*. **2** (2023) 67–71. https://doi.org/10.56425/cma.v2i3.65.

[38] F. Tezcan, A. Mahmood, G. Kardaş, The investigation of Cu2O electrochemical deposition time effect on ZnO for water splitting, *J Mol Struct*. **1193** (2019) 342–347. https://doi.org/10.1016/J.MOLSTRUC.2019.05.052.

[39] S. Budi, M. Takahashi, M.G. Sutrisno, W.A. Adi, Z. Fairuza, B. Kurniawan, S. Maenosono, A.A. Umar, Phases evolution and photocatalytic activity of Cu2O films electrodeposited from a non-pH-adjusted solution, *R Soc Open Sci*. **10** (2023). https://doi.org/10.1098/RSOS.230247.

[40] W. Chen, Y. Wang, S. Liu, L. Gao, L. Mao, Z. Fan, W. Shangguan, Z. Jiang, Non-noble metal Cu as a cocatalyst on TiO2 nanorod for highly efficient photocatalytic hydrogen production, *Appl Surf Sci*. **445** (2018) 527–534. https://doi.org/10.1016/J.APSUSC.2018.03.209.

[41] Y. Cheng, Y. Lin, J. Xu, J. He, T. Wang, G. Yu, D. Shao, W.H. Wang, F. Lu, L. Li, X. Du, W. Wang, H. Liu, R. Zheng, Surface plasmon resonance enhanced visible-light-driven photocatalytic activity in Cu nanoparticles covered Cu2O microspheres for degrading organic pollutants, *Appl Surf Sci*. **366** (2016) 120–128. https://doi.org/10.1016/J.APSUSC.2015.12.238.

[42] A. Ait Hssi, L. Atourki, N. Labchir, M. Ouafi, K. Abouabassi, A. Elfanaoui, A. Ihlal, S. Benmokhtar, K. Bouabid, High-quality Cu2O thin films via electrochemical synthesis under a variable applied potential, *Journal of Materials Science: Materials in Electronics*. **31** (2020) 4237–4244. https://doi.org/10.1007/S10854-020-02976-W/METRICS.

[43] A. Maddu, V. Lestari, M.N. Indro, Influence of Applied Potential on The Structural and Optical Properties of Cu2O Thin Films Grown by Electrochemical Deposition, *Jurnal Sains Materi Indonesia*. **24** (2022) 16–23. https://doi.org/10.17146/jsmi.2022.24.1.6709.

[44] X. Jiang, M. Zhang, S. Shi, G. He, X. Song, Z. Sun, Influence of Applied Potential on the Band Gap of Cu/Cu 2 O Thin Films , *J Electrochem Soc*. **161** (2014) D640–D643. https://doi.org/10.1149/2.0181412JES/XML.

[45] A. Bahdaouia, S. Amara, L. Adnane, S. Columbus, K. Daoudi, A. Mahieddine, Synthesis, characterization and photo-electrochemical properties of novel Cu(Cr1-,Al)2O4 spinel oxides for enhanced photodegradation of organic dyes under UV light, *Int J Hydrogen Energy*. **47** (2022) 9301–9318. https://doi.org/10.1016/j.ijhydene.2022.01.016.

[46] X.-J. Lv, S.-X. Zhou, C. Zhang, H.-X. Chang, Y. Chen, W.-F. Fu, Synergetic effect of Cu and graphene as cocatalyst on TiO2 for enhanced photocatalytic hydrogen evolution from solar water splitting, *J Mater Chem*. **22** (2012) 18542. https://doi.org/10.1039/c2jm33325b.

[47] M.G. Sutrisno, Yusmaniar, A.M. Noor, S. Budi, Electrodeposition of Zn-Doped Cu2O-Cu/Ni for methylene blue photodegradation, *J Phys Conf Ser*. **2596** (2023) 012017. https://doi.org/10.1088/1742-6596/2596/1/012017.

[48] J. Zhou, Y. Li, L. Yu, Z. Li, D. Xie, Y. Zhao, Y. Yu, Facile in situ fabrication of Cu2O@Cu metal-semiconductor heterostructured nanorods for efficient visible-light driven CO2 reduction, *Chemical Engineering Journal*. **385** (2020) 123940. https://doi.org/10.1016/j.cej.2019.123940.

[49] R.S. Dariani, A. Esmaeili, A. Mortezaali, S. Dehghanpour, Photocatalytic reaction and degradation of methylene blue on TiO2 nano-sized particles, *Optik (Stuttg)*. **127** (2016) 7143–7154. https://doi.org/10.1016/j.ijleo.2016.04.026.

[50] Y.J. Jang, C. Simer, T. Ohm, Comparison of zinc oxide nanoparticles and its nano-crystalline particles on the photocatalytic degradation of methylene blue, *Mater Res Bull*. **41** (2006) 67–77. https://doi.org/10.1016/j.materresbull.2005.07.038.

[51] S. Budi, M.G. Sutrisno, Y. Pratiwi, Yusmaniar, Enhanced photocatalytic activity of CoNi-decorated Zn-doped Cu 2 O synthesized by electrodeposition technique, *Mater Adv*. **4** (2023) 1081–1088. https://doi.org/10.1039/D2MA00916A.

[52] Z. Li, J. Liu, D. Wang, Y. Gao, J. Shen, Cu2O/Cu/TiO2 nanotube Ohmic heterojunction arrays with enhanced photocatalytic hydrogen production activity, *Int J Hydrogen Energy*. **37** (2012) 6431–6437. https://doi.org/10.1016/J.IJHYDENE.2012.01.075.